PHYSICAL REVIEW D **79,** 115009 (2009)

Neutralino reconstruction in supersymmetry with long-lived staus

Sanjoy Biswas* and Biswarup Mukhopadhyaya†

Regional Centre for Accelerator-based Particle Physics, Harish-Chandra Research Institute, Chhatnag Road, Jhunsi, Allahabad - 211 019, India

(Received 28 February 2009; published 15 June 2009)

We consider a supergravity scenario, with universal scalar and gaugino masses at high scale, with a right-chiral neutrino superfield included in the spectrum. Such a scenario can have the lightest supersymmetric particle (LSP) dominated by the right sneutrino and a stau as the next-to lightest supersymmetric particle (NLSP). Since decays of all particles into the LSP are suppressed by the neutrino Yukawa coupling, the signal of supersymmetry consists of charged tracks of stable particles in the muon chamber. We demonstrate how a neutralino decaying into a tau and the stau NLSP can be fully reconstructed over substantial areas in the supergravity parameter space. We also suggest event selection criteria for eliminating backgrounds, including combinatorial ones, and use a new method for the extraction of the mass of the stau NLSP, using its three-momentum as obtained from the curvature of the charged track.

DOI: 10.1103/PhysRevD.79.115009 PACS numbers: 12.60.Jv

I. INTRODUCTION

Searches for supersymmetry (SUSY) [1–3] at the Large Hadron Collider (LHC) are largely based on signals with missing transverse energy ($\not{E}_T$). This is because SUSY, in its $\mathcal{R}$-parity conserving form (with $\mathcal{R}$ parity defined by $\mathcal{R} = (-)^{3B+L+2S}$), offers the lightest supersymmetric particle (LSP) which is stable, and, if electrically uncharged and weakly interacting, is potentially a cold dark matter candidate. The lightest neutralino (χ_1^0) turns out to be the LSP in most theoretical models. All SUSY cascades at collider experiments should culminate in the pair production of the LSP within the detector itself. The neutral and nonstrongly interacting character of the LSP results in its invisibility at colliders, and thus a large energy-momentum imbalance, together with energetic jets and/or leptons emerges as the characteristic signal of SUSY containing a dark matter candidate.

It should be remembered, though, that the above possibility is not unique. Apart from the lightest neutralino, the left-chiral sneutrinos in the minimal SUSY standard model (MSSM) can in principle be a dark matter candidate as well. This is, however, strongly disfavored by direct dark matter search experiments, because the SU(2) interaction of a left-chiral sneutrino [as opposed to the U(1) or Yukawa dominated interaction of a neutralino] gives rise to unacceptably large cross sections of elastic scattering with dark matter detectors. In addition, a left-chiral sneutrino LSP is difficult to accommodate in a scenario where the SUSY breaking masses evolve from ''universal'' scalar and gaugino mass parameters at a high scale [4].

The situation changes if one has right-chiral neutrino superfields in addition, a possibility that often haunts us as evidence piles up in favor of neutrino masses and mixing [5,6]. It has been shown in some recent works [7] that such a right-chiral sneutrino may pass off as a dark matter candidate without any contradiction from available data [8]. Since the right-chiral sneutrino has no gauge interaction, the only way it can interact with matter is via neutrino Yukawa coupling, the strength of its interaction is too feeble to be seen in dark matter search experiments. In such a case, the next-to-lightest SUSY particle (NLSP), too, has an excruciatingly slow rate of decay into the LSP dominated by right-chiral sneutrino states. Consequently, the NLSP is stable on the scale of collider detectors, and, in cases where it is a charged particle, the essence of the SUSY signal lies not in $\not{E}_T$ but in charged tracks due to massive particles seen in the muon chambers.

Such stable charged particles can in principle be distinguished from muons through a number of techniques. These include the measurement of time delay between the inner tracking chamber and the muon chamber, the degree of ionization, and also more exotic proposals such as the absorption of the stable particles in a chamber which can be subsequently emptied underground to observe the decays [9]. While these are all of sufficient importance and interest, some of us have shown in earlier works [10,11] that there are some very good kinematic discriminators for such stable charged particles, which make the signals practically background free for both stau and stop NLSP. Event selection criteria based on the transverse momentum p_T of the tracks, in conjuction with quantities such as the scalar sum of all visible transverse momenta and the invariant mass of track pairs, are found to be useful in this respect. In this work, we perform a detailed simulation of signals, backgrounds, and mistags to show that the masses of neutralinos can be reconstructed to a high level of precision for a scenario with $\tilde{\tau}$ NLSP and an LSP dominated by the right-chiral sneutrino of the third family. We

*sbiswas@mri.ernet.in
†biswarup@mri.ernet.in

use the technique of tau reconstruction for this purpose. Also, we depend on neither ionization nor time delay for extracting the mass of the stable stau, but rather obtain it using an algorithm that depends on event-by-event information on two taus and two stable tracks in the final state.

It should be mentioned that the signal discussed here as well as the reconstruction technique advocated by us is not limited to scenarios with right-sneutrino LSP alone. One can have stable staus in SUSY, when, for example, one has a gravitino LSP in a supergravity (SUGRA) model [12]. They can be envisioned in gauge-mediated SUSY breaking theories as well [13]. In the MSSM, too, one can have the so-called coannihilation region of dark matter, where a stau and the neutralino LSP are closely degenerate, leading to a quasistable character of the former [14]. It should be emphasized that our suggested procedure is applicable to all of these cases. What we find as a bonus is that scenarios with stau NLSP and right-sneutrino LSP occur rather naturally in a SUGRA model [7,10] with a universal scalar mass which is the origin of the right-sneutrino mass as well. Thus the mere addition of a right-sneutrino superfield, which is perhaps the most minimal input to explain neutrino masses, can turn a mSUGRA theory into one with a stau NLSP and a sneutrino LSP. Thus one can identify regions in the $m_0 - M_{1/2}$ plane of the theory, where the reconstruction of unstable neutralinos is feasible at the LHC.

In Sec. II, we discuss the scenario under investigation as well as the super particle spectrum and motivate the choice of benchmark points used for demonstrating our claims, in the context of a supergravity scenario. The signal looked for, the corresponding standard model backgrounds, and the event selection criteria chosen by us are discussed in Sec. III. Section IV contains discussions on the various steps in reconstructing neutralinos. The regions in the $m_0 - M_{1/2}$ plane in a SUGRA scenario, where neutralino reconstruction is possible in our method, are also pointed out in this section. We summarize and conclude in Sec. V.

II. RIGHT-SNEUTRINO LSP IN SUPERGRAVITY

The superpotential of the MSSM [15] is given (suppressing family indices) by

$$W_{\rm MSSM} = y_l \hat{L}\hat{H}_d\hat{E}^c + y_d\hat{Q}\hat{H}_d\hat{D}^c + y_u\hat{Q}\hat{H}_u\hat{U}^c + \mu\hat{H}_d\hat{H}_u, \quad (1)$$

where $\hat{H}_d$ and $\hat{H}_u$, respectively, are the Higgs superfields that give mass, respectively, to the $T_3 = -1/2$ and $T_3 = +1/2$ fermions. y's are the strengths of Yukawa interactions. $\hat{L}$ and $\hat{Q}$ are the left-handed lepton and quark superfields, respectively, whereas $\hat{E}^c$, $\hat{D}^c$, and $\hat{U}^c$, in that order, are the right-handed gauge singlet charged lepton, and down-type and up-type quark superfields. μ is the Higgsino mass parameter.

As already mentioned, the MSSM must be additionally equipped to explain nonvanishing neutrino masses. Phenomenologically, the simplest (though not theoretically the most satisfying) way to do so is to assume neutrinos to be of a Dirac type and simply add one right-handed neutrino superfield to each family. The superpotential of the minimal SUSY standard model is thus extended by just one term per family, of the form

$$W_\nu^R = y_\nu \hat{H}_u \hat{L}\hat{\nu}_R^c. \quad (2)$$

However, having such small Dirac masses for the neutrinos would imply that the neutrino Yukawa couplings (y_ν) are quite small ($\sim 10^{-13}$). The above term in the superpotential obviously implies the inclusion of right-handed sneutrinos in the (super)particle spectrum, and these sneutrinos will have all their interactions proportional to the corresponding neutrino masses. Thus the dominantly right-handed eigenstate of the tau sneutrino might become a viable dark matter candidate, without coming into conflict with dark matter search limits, thanks to its extremely feeble strength of interaction with all matter.

Interestingly, scenarios where the MSSM is embedded in a bigger, high-scale framework for SUSY breaking can support the above situation. The most commonly invoked scheme is minimal supergravity (mSUGRA) where all scalar (gaugino) masses at low energy arise from a universal mass parameter $m_0(M_{1/2})$ at a high scale where supergravity, or local SUSY, is broken. If one adds a right-chiral neutrino superfield, then the right-sneutrino mass may be assumed to originate in the same parameter m_0. As we shall see below, this causes the physical state dominated by the right-chiral sneutrino to become the LSP. It has been shown that such a possibility is consistent with all experimental bounds [16] and also compatible with the dark matter density in the Universe [7,8].

The neutrinos masses can be schematically shown as

$$m_\nu = y_\nu \langle H_u^0 \rangle = y_\nu v \sin\beta, \quad (3)$$

where $\tan\beta$ is the ratio of the vacuum expectation values of the two Higgs doublets that give masses to the up- and down-type quarks, respectively. The actual mass eigenvalues will of course depend on the Yukawa coupling matrix. This, however, does not affect the collider signals of the SUSY scenario under consideration here, as the interaction strengths of the dominantly right-chiral states are always very small in magnitude.

Upon inclusion of right-chiral neutrino superfield into the SUGRA framework, the superparticle spectrum mimics the mSUGRA spectrum in all details except for the identity of the LSP. As already mentioned, SUSY breaking in the hidden sector at high scale is manifested in universal soft masses for scalars (m_0) and gauginos ($M_{1/2}$), together with the trilinear (A) and bilinear (B) SUSY breaking parameters in the scalar sector (of which the latter is determined by electroweak symmetry breaking

conditions). Masses for squarks, sleptons, and gauginos, all the mass parameters in the Higgs sector as well as the Higgsino mass parameter μ (up to a sign) are determined, once the high scale of SUSY breaking in the hidden sector ($\mathcal{O} \sim 10^{11}$ GeV) is specified. Neglecting interfamily mixing, the mass terms for sneutrinos arising in this manner are given by

$$-\mathcal{L}_{\text{soft}} \sim M^2_{\tilde{\nu}_R}|\tilde{\nu}_R|^2 + (y_\nu A_\nu H_u \cdot \tilde{L}\tilde{\nu}^c_R + \text{H.c.}), \quad (4)$$

where A_ν is the term driving left-right mixing in the scalar mass matrix and is obtained by running of the trilinear soft SUSY breaking term A [17]. The Yukawa couplings can cause large splitting in the third-family squark and sleptons masses while the first two families are more closely degenerate. On the other hand, the degree of left-right mixing of sneutrinos, driven largely by the Yukawa couplings, is extremely small.

The sneutrino mass-squared matrix is thus of the form

$$m^2_{\tilde{\nu}} = \begin{pmatrix} M^2_{\tilde{L}} + \frac{1}{2}m^2_Z \cos 2\beta & y_\nu v(A_\nu \sin\beta - \mu\cos\beta) \\ y_\nu v(A_\nu \sin\beta - \mu\cos\beta) & M^2_{\tilde{\nu}_R} \end{pmatrix}, \quad (5)$$

where $M_{\tilde{L}}$ is the soft scalar mass for the left-handed sleptons, whereas the $M_{\tilde{\nu}_R}$ is that for the right-handed sneutrino. In general, $M_{\tilde{L}} \neq M_{\tilde{\nu}_R}$ because of their different evolution patterns. In addition, the D-term contribution for the former causes a difference between the two diagonal entries. While the evolution of all other parameters in this scenario is practically the same as in the MSSM, the right-chiral sneutrino mass parameter evolves [18] at the one-loop level as

$$\frac{dM^2_{\tilde{\nu}_R}}{dt} = \frac{2}{16\pi^2} y^2_\nu A^2_\nu. \quad (6)$$

Clearly, the extremely small Yukawa couplings cause $M_{\tilde{\nu}_R}$ to remain nearly frozen at the value m_0, whereas the other sfermion masses are enhanced at the electroweak scale. Thus, for a wide range of values of the gaugino mass, one naturally has sneutrino LSPs, which, for every family, are dominated by the right-chiral state:

$$\tilde{\nu}_1 = -\tilde{\nu}_L \sin\theta + \tilde{\nu}_R \cos\theta. \quad (7)$$

The mixing angle θ is given as

$$\tan 2\theta = \frac{2y_\nu v \sin\beta|\cot\beta\mu - A_\nu|}{m^2_{\tilde{\nu}_L} - m^2_{\tilde{\nu}_R}}, \quad (8)$$

which is suppressed by y_ν, especially if the neutrinos have Dirac masses only. It is to be noted that all three (dominantly) right sneutrinos have a similar fate here, and one has near degeneracy of three such LSPs. However, of the three charged slepton families, the amount of left-right mixing is always the largest in the third (being, of course, more pronounced for large $\tan\beta$), and the lighter stau ($\tilde{\tau}_1$) often turns out to be the NLSP in such a scenario.[1]

Thus the mSUGRA parameter set [m_0, $M_{1/2}$, A_0, sign(μ), and $\tan\beta$] in an $\mathcal{R}$-parity conserving scenario can eminently lead to a spectrum where all three generations of right sneutrinos will be either stable or metastable but very long lived and can lead to different decay chains of supersymmetric particles, as compared to those with a neutralino LSP. However, as we shall see below, the deciding factor is the lighter sneutrino mass eigenstate of the third family, so long as the state $\tilde{\tau}_1$ is the lightest among the charged sleptons.

All superparticles will have to decay into the lighter sneutrino of a particular family via either gauge interactions (such as $\tilde{\tau}_L \to W\tilde{\nu}^\tau{}_1$) or a Yukawa coupling (such as $\tilde{l}_L \to H^-\tilde{\nu}_1$ or $\tilde{\nu}_2 \to h^0\tilde{\nu}_1$). In the former case, the decay depends entirely on the $\tilde{\nu}_L$ content of $\tilde{\nu}_1$, which again depends on the neutrino Yukawa coupling. The same parameter explicitly controls the decay in the latter case, too. Therefore, while the lighter sneutrinos of the first two families can in principle be produced from decays of the corresponding charged sleptons, such decays will be always suppressed compared to even three-body decays such as $\tilde{e}_1(\tilde{\mu}_1) \to e(\mu)\bar{\tau}\tilde{\tau}_1$ (when the sleptons are lighter than all neutralinos). For the $\tilde{\tau}$ NLSP, however, the only available decay channel is $\tilde{\tau}_1 \to W(H^-)\tilde{\nu}_1$, with either real or virtual charged Higgs. Both of these decay channels are driven by the extremely small neutrino Yukawa coupling.

This causes the NLSP to be a long-lived particle and opens up a whole set of new possibilities for collider signatures for such long-lived particles, while retaining contributions to dark matter from the sneutrino LSP. The NLSP appears stable in collider detectors and gives highly ionizing charged tracks.

Apart from a stau, the NLSP could be a chargino, a stop, or a sbottom. The former is in general difficult to achieve in a scenario where the chargino and neutralino masses are determined by the same set of electroweak gaugino and Higgsino masses. The phenomenology of the long-lived stop NLSP [19], the likelihood of the corresponding signals being available at the early phase of the LHC, and the potential for the reconstruction of gluino masses have been discussed in an earlier work [11]. The stau NLSP, as we shall see below, offers a new opportunity to reconstruct both the lightest and second lightest neutralino masses.

It may be noted here that the region of the mSUGRA parameter space where we work is consistent with all experimental bounds, including both collider and low-energy constraints (such as the LEP and Tevatron con-

[1]We have neglected interfamily mixing in the sneutrino sector in this study. While near-degenerate physical states make such mixing likely, the degree of such mixing is model dependent and does not generally affect the fact that all cascades culminate in the lighter stau, so long as the latter is the NLSP, which is the scenario studied here.

straints on the masses of Higgs, gluinos, charginos and so on as well as those from $b \to s\gamma$, correction to the ρ parameter, $(g_\mu - 2)$, etc.). Our choice of parameters in the $m_0 - M_{1/2}$ plane would correspond to a stau LSP without the right sneutrino in the (super) particle spectrum. Such a situation would have been ruled out, had not the existence of the right-chiral neutrino superfield, with the right sneutrino at the bottom of the spectrum, been assumed [20]. However with the right sneutrino as the LSP, we find this choice to be a preferable and well-motivated option. The $\tilde{\nu}_1$ LSP arising out of such a choice becomes a viable dark matter candidate, though not necessarily the only one. Using the formulas given by Asaka *et al.* in Ref. [7], the contribution to the relic density (Ωh^2) is found to be about 1 order of magnitude below the acceptable value [8]. While this leaves room for additional sources of dark matter, the scenario presented here is consistent from the viewpoint of overclosure of the Universe.

We focus on both the regions where (a) $m_{\tilde{\tau}_1} > m_{\tilde{\nu}_1} + m_W$, and (b) the above inequality is not satisfied. In the first case, the dominant decay mode is the two-body decay of the NLSP, $\tilde{\tau}_1 \to \tilde{\nu}_1 W$, and, in the second, the decay takes place via a virtual W. However, the decay takes place outside the detector in both cases. Decays into a charged Higgs constitute a subdominant channel for the lighter stau.

Furthermore, we try to identify regions of the parameter space, where neutralinos decaying into a tau and a stau can be reconstructed, through the reconstruction of the tau and the detection of the stau in the muon chamber. The rates for electroweak production of neutralinos are generally rather low for this process. Therefore, the procedure works better when neutralinos are produced from the cascade decays of squarks and gluinos. This is in spite of the additional number of jets in such processes, which may fake the tau in certain cases and complicate the analysis of the signals. We are thus limited to those regions of the parameter space, where the gluino and squark production rates are appreciable, and therefore the value of $M_{1/2}$ is not too high.

With all the above considerations in mind, we concentrate on the lighter *stau* ($\tilde{\tau}_1$) to be the NLSP with lifetime large enough to penetrate collider detectors like the muons themselves. Using the spectrum generator of ISAJET 7.78 [21], we find that a large mSUGRA parameter space can realize this scenario of a right-sneutrino LSP and stau NLSP, provided that $m_0 < m_{1/2}$ and one has $\tan\beta$ in the range $\gtrsim 25$, the latter condition being responsible for a larger left-right off-diagonal term in the stau-mass matrix (and thus one smaller eigenvalue). In Table I we identify a few benchmark points, all within a SUGRA scenario with universal scalar and gaugino masses, characterized by long-lived staus at the LHC.

In the next section we use these benchmark points to discuss the signatures of the stau NLSP at the LHC and look for the final states in which it is possible to reconstruct the neutralinos.

III. SIGNAL AND BACKGROUNDS

The signal which we have studied as a signature of stau NLSP and motivated by the possible reconstruction of the neutralinos from the final state, is given by

$$2\tau_j + 2\tilde{\tau}(\text{charged track}) + \not{E}_T + X,$$

where τ_j denotes a jet out of a one-prong decay of the tau,

TABLE I. Proposed benchmark points (BP) for the study of the stau-NLSP scenario in the SUGRA with right-sneutrino LSP. The values of m_0 and $M_{1/2}$ are given in GeV. We have also set $A_0 = 100$ GeV and $\text{sgn}(\mu) = +$ for benchmark points under study.

Input	BP-1	BP-2	BP-3	BP-4	BP-5	BP-6
mSUGRA	$m_0 = 100$ $m_{1/2} = 600$ $\tan\beta = 30$	$m_0 = 100$ $m_{1/2} = 500$ $\tan\beta = 30$	$m_0 = 100$ $m_{1/2} = 400$ $\tan\beta = 30$	$m_0 = 100$ $m_{1/2} = 350$ $\tan\beta = 30$	$m_0 = 100$ $m_{1/2} = 325$ $\tan\beta = 30$	$m_0 = 100$ $m_{1/2} = 325$ $\tan\beta = 25$
$m_{\tilde{e}_L}$, $m_{\tilde{\mu}_L}$	418	355	292	262	247	247
$m_{\tilde{e}_R}$, $m_{\tilde{\mu}_R}$	246	214	183	169	162	162
$m_{\tilde{\nu}_{eL}}$, $m_{\tilde{\nu}_{\mu L}}$	408	343	279	247	232	232
$m_{\tilde{\nu}_{\tau L}}$	395	333	270	239	224	226
$m_{\tilde{\nu}_{iR}}$	100	100	100	100	100	100
$m_{\tilde{\tau}_1}$	189	158	127	112	106	124
$m_{\tilde{\tau}_2}$	419	359	301	273	259	255
$m_{\chi_1^0}$	248	204	161	140	129	129
$m_{\chi_2^0}$	469	386	303	261	241	240
$m_{\chi_1^\pm}$	470	387	303	262	241	241
$m_{\tilde{g}}$	1362	1151	937	829	774	774
$m_{\tilde{t}_1}$	969	816	772	582	634	543
$m_{\tilde{t}_2}$	1179	1008	818	750	683	709
m_{h^0}	115	114	112	111	111	111

$\not{E}_T$ stands for missing transverse energy, and all accompanying hard jets arising from cascades are included in X.

We have simulated pp collisions with a center-of-mass energy $E_{\text{c.m.}} = 14$ TeV. The prediction of events assumes an integrated luminosity of 300 fb^{-1}. The signal and various backgrounds are calculated using PYTHIA (Version 6.4.16) [22]. Numerical values of various parameters, used in our calculation, are as follows [16]:

$$M_Z = 91.2 \text{ GeV}, \quad M_W = 80.4 \text{ GeV},$$
$$M_t = 171.4 \text{ GeV}, \quad M_H = 120 \text{ GeV},$$
$$\alpha_{em}^{-1}(M_Z) = 127.9, \quad \alpha_s(M_Z) = 0.118.$$

We have worked with the CTEQ5L parton distribution function [23]. The factorization and renormalization scale are set at $\mu_F = \mu_R = m_{\text{average}}^{\text{final}}$. In order to make our estimate conservative, the signal rates have not been multiplied by any K factor [24], while the main background, namely, that from $t\bar{t}$ production, has been multiplied by a K factor of 1.8 [25]. The effects of initial state radiation and final state radiation have been considered in our study.

A. Signal subprocesses

We have studied all SUSY subprocess leading to the desired final states. Neutralinos are mostly produced in cascade decays of strongly interacting sparticles. The dominant contributions thus come from

(i) gluino pair production: $pp \to \tilde{g}\,\tilde{g}$;
(ii) squark pair production: $pp \to \tilde{q}_i\tilde{q}_j$, $\tilde{q}_i\tilde{q}_i^*$;
(iii) associated squark-gluino production: $pp \to \tilde{q}\,\tilde{g}$.

In addition, electroweak pair production of neutralinos can also contribute to the signal we are looking for. The rates are, however, much smaller (see Table II). Moreover, the relatively small masses of the lightest and the second lightest neutralinos (as compared to the squarks and the gluino) cause the signal from such subprocesses to be drastically reduced by the cut employed by us on the scalar sum of all visible p_T's. For example, for benchmark point 1 (BP1), one has less than 5% of the total contribution from electroweak processes.

The production of squarks and gluinos has potentially large cross sections at the LHC. For all our benchmark points listed in Table I, the gluino is heavier than the squarks. Thus its dominant decay is into a squark and a quark. χ_1^0 being mostly $\tilde{B}$ dominated the main contribution to χ_1^0 production comes from the decay of right-handed squarks ($\tilde{q}_R$) and its decay branching ratio into the $\tilde{\tau}$-τ pair is almost 100% when it is just above the lighter stau in the spectrum. On the other hand, the χ_2^0 is mostly $\tilde{W}_3$ dominated, and therefore the main source of its production is cascade decay of left-chiral squarks ($\tilde{q}_L$). Such a χ_2^0 can also decay into a $\tilde{\tau}$-τ pair.

If one can obtain complete information on the four-momentum of the $\tilde{\tau}$ and the τ, it is thus possible to reconstruct both χ_1^0 and χ_2^0 using the final state mentioned above. The other two heavier neutralinos (χ_3^0 and χ_4^0), due to their low production rate and small decay branching ratios into the $\tilde{\tau}$-τ pair, are relatively difficult to reconstruct.

TABLE II. The number of $2\tau_j + 2\tilde{\tau}$(charged track) $+ \not{E}_T + X$ events, satisfying our basic cuts, for $\int Ldt = 300$ GeV, from various channels.

Subprocesses	BP-1	BP-2	BP-3	BP-4	BP-5	BP-6
All SUSY	1765	4143	11 726	20 889	28 864	15 439
$\tilde{q}\tilde{q}^*$, $\tilde{g}\,\tilde{g}$, $\tilde{q}\,\tilde{g}$	1616	3897	11 061	19 765	27 785	14 426

B. Background subprocesses

The standard model background to $2\tau_j + 2\tilde{\tau} + \not{E}_T$ comes mainly from the following subprocesses:

(i) $t\bar{t}$ production, $t\bar{t} \to bWbW$: Where two of the resulting jets can be faked as a tau jet, and muons can come from the W's. One can also have a situation in which any (or both) of the b quark decays semileptonically ($b \to c\mu\nu_\mu$) and any (or both) of the W decays to the τ-ν_τ pair. Though the efficiency of a non-tau jet being identified as a narrow taulike jet is small (as will be discussed in a later section), and it is very unlikely to have isolated muons from semileptonic decays of the b, the overwhelmingly large number of $t\bar{t}$ events produced at the LHC makes this subprocess quite a serious source of backgrounds.
(ii) Z^0-pair production, $ZZ \to 2\tau + 2\mu$: This subprocess also gives an additional contribution to the background, when one Z decays into a $\tau\tau$ pair and the other one into a pair of muons.
(iii) Associated ZH production, $ZH \to 2\tau + 2\mu$: This subprocess, though having a small cross section, can contribute to the background through the decay of $H \to \tau\tau$ and $Z \to \mu\mu$, which can fake our signal as well.

The additional backgrounds from $t\bar{t}W$, $t\bar{t}Z$, and Z + jets can be suppressed by the same cuts as those described below. Also a higher non-tau-jet rejection factor and Z invariant mass cut can reduce the $t\bar{t}Z$ and Z + jets backgrounds considerably.

C. Event selection criteria

In selecting the candidate events selected for neutralino reconstruction, we choose the two highest-p_T isolated charged tracks showing up in the muon chamber, both with $p_T > 100$ GeV, as stable staus. (See the detailed discussion later in this section.) The isolation criteria for the tracks are shown in Table III. In addition to the p_T cut, the scalar sum of all jets and lepton in each event is required to be greater than 1 TeV. It is clear from Figs. 1 and 2 that the standard model backgrounds are effectively

TABLE III. Cuts applied for event selection, background elimination, and neutralino reconstruction.

Cuts	
Basic cuts	$p_T^{\text{lep,stau}} > 10$ GeV, $p_T^{\text{hardest jet}} > 75$ GeV, $p_T^{\text{other jets}} > 50$ GeV, 40 GeV $< \not{E}_T < 150$ GeV, $\lvert\eta\rvert < 2.5$ for leptons, jets, & stau $\Delta R_{ll} > 0.2$, $\Delta R_{lj} > 0.4$, $\Delta R_{\tilde{\tau}l} > 0.2$, $\Delta R_{\tilde{\tau}j} > 0.4$, $\Delta R_{jj} > 0.7$
Cuts for background elimination	$p_T^{\text{isocharge track}} > 100$ GeV, $\Sigma\lvert\vec{p}_T\rvert > 1$ TeV
Invariant mass difference of two nearby pairs	$\lvert M_{\tilde{\tau}\tau}^{\text{pair1}} - M_{\tilde{\tau}\tau}^{\text{pair2}}\rvert < 50$ GeV

eliminated through the above criteria. In addition, we require two τ jets with $p_T > 50$ GeV and $\not{E}_T > 40$ GeV for each event. The justification for both of these cuts is provided when we discuss τ tagging and reconstruction.

The identification and 3-momentum reconstruction of the charged track at the muon chamber is done following the same criteria and procedure as those for muons.

In order to obtain the invariant mass of a tau-stau pair, one needs to extract information on the mass of the stable charged particle (the stau in our context). While standard techniques such as time delay measurement or the degree of ionization produced has been suggested in a number of earlier works [26], we extract mass information from an event-by-event analysis which is reported in the next section. The efficiency for the reconstruction of staus has been taken to be the same as that of muons with $p_T > 10$ GeV in the pseudorapidity range $\lvert\eta\rvert < 2.5$, and is set at 90% following [27].

1. τ-jet tagging and τ reconstruction

τ-jet identification and τ reconstruction are necessary for both background reduction and mass reconstruction of the neutralinos. We have concentrated on hadronic decays of the τ in the one-prong channel.[2] These are jetlike clusters in the calorimeter containing a relatively small number of charged and neutral hadrons. A τ decays hadronically about 65% of the time, producing a τ jet. The momentum of such a jet in the plane transverse to the parent τ is small compared to the τ energy, so long as the p_T of the τ jet is large compared to the τ mass. In this limit, hadronic τ decays produce narrow jets collinear with the parent τ. The neutrinos that carry missing E_T also have the same direction in this limit. This gives one a handle in reconstructing the τ's, if one selects events where no other invisible particle is likely to be produced.

Given the masses of the SUSY particles in our benchmark scenarios, the τ's produced out of neutralino decay are hard enough, so that one can simulate τ decays in the collinear approximation described above. A detailed discussion on the procedure followed for complete reconstruction of a pair of τ's is found in [28]. We have selected hadronic jets with $E_T > 50$ GeV as candidate products of τ decay. A rather conservative non-tau jet rejection factor of 20 has been assumed, while the identification efficiency of a true τ jet has been assumed to be 50% following [29,30].

To describe the procedure in brief, one can fully reconstruct the τ by knowing $x_{\tau_{hi}}$ $(i = 1, 2)$, the fractions of the parent τ energy carried by each product jet. The two unknowns can be solved from the two components of the missing transverse momentum ($\vec{\not{p}}_T$) of a particular event.

If $p_{\tau_i}^{\mu}$, p_{hi}^{μ} are, respectively, the components of four-momentum of the parent τ and the collinear jet produced from it $(i = 1, 2)$, then

$$p_{hi}^{\mu} = x_{\tau_{hi}} p_{\tau_i}^{\mu} \qquad (\mu = 0, 1, \ldots, 4) \tag{9}$$

(as $E_\tau \approx \lvert\vec{p}_\tau\rvert$, in the limit $m_\tau \to 0$) and one can write

$$\vec{\not{p}}_T = \left(\frac{1}{x_{\tau_{h1}}} - 1\right)\vec{p}_{h1} + \left(\frac{1}{x_{\tau_{h2}}} - 1\right)\vec{p}_{h2}. \tag{10}$$

This yields two conditions for $x_{\tau_{hi}}$. Solving them, one obtains the τ four-momenta as $p_{hi}/x_{\tau_{hi}}$. In practice, as will be discussed below, the recorded missing momentum, $\vec{\not{p}}_T^{\text{rec}}$, is different from the true one, namely, $\vec{\not{p}}_T^{\text{true}}$. This error can lead to unphysical solutions for the reconstructed τ momenta in some cases. Such a situation often arises when the two taus are produced back to back. This in turn means that the τ neutrinos are also produced back to back in the collinear approximation. This reduces the magnitude of $\vec{\not{p}}_T$, when errors due to mismeasurements can lead to unphysical solutions. This is sometimes avoided by leaving out back-to-back orientation of the two τ-jet candidates, with some tolerance. In our analysis, a minimum value for $\not{E}_T$ (≈ 40 GeV) and positivity of $x_{\tau_{hi}}$'s have been imposed as necessary conditions, in order to minimize the number of unphysical solutions. Besides, $p_T > 50$ GeV for each τ jet ensures the validity of the collinear approximation in τ decays. The τ-identification efficiency and the jet rejection factor are also better optimized with this p_T cut [29,30].

Of course, with a jet rejection factor of $1/20$, one cannot rule out the possibility of QCD jets masquerading as τ's, in view of the huge number of QCD events at the LHC. Such fakes constitute irreducible backgrounds to the τ-reconstruction procedure. However, as we shall see in the numerical results presented in the next section, triggering on the rather strikingly spectacular properties of the

[2]We have not considered the leptonic decay of tau, as it is difficult to identify lepton coming from tau decay to that coming from cascade decay of other objects like heavy quarks or W's.

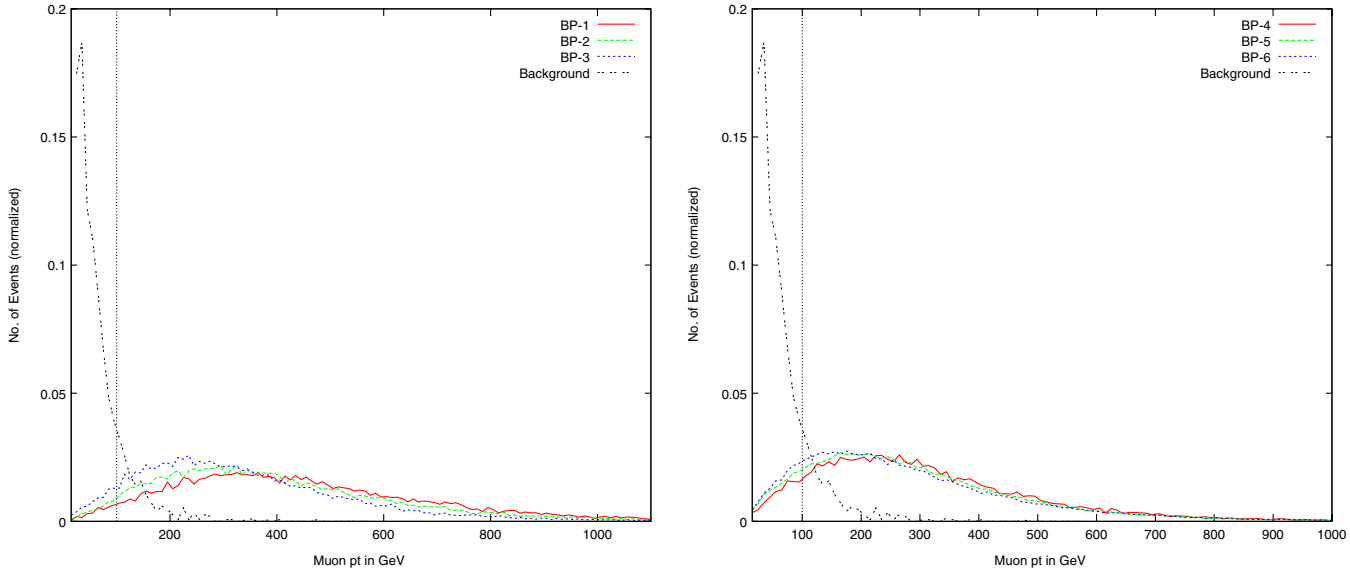

FIG. 1 (color online). p_T distribution (normalized to unity) of the muonlike track (harder) for the signal and the background, for all benchmark points. The vertical lines indicate the effects of a p_T cut at 100 GeV.

quasistable stau pair enables one to filter out the genuine events in the majority of cases.

2. Reconstruction of $\vec{\not{p}}_T$

It is evident from the above observations that the reconstruction of $\vec{\not{p}}_T$ is very crucial for our study. The reconstructed $\vec{\not{p}}_T$ differs considerably from true $\vec{\not{p}}_T$, due to several reasons. The $\vec{\not{p}}_T^{\text{true}}$ is related to the experimentally reconstructed $\vec{\not{p}}_T^{\text{rec}}$ by the following relation:

$$\vec{\not{p}}_T^{\text{rec}} = \vec{\not{p}}_T^{\text{true}} + \vec{\not{p}}_T^{\text{Forw}} + \vec{\not{p}}_T^{<0.5}, \tag{11}$$

where $\vec{\not{p}}_T^{\text{Forw}}$ corresponds to the total transverse momentum carried by the particles escaping detection in the range $|\eta| > 5$ and $\vec{\not{p}}_T^{<0.5}$ corresponds to the total transverse momentum carried by the particles in the range $|\eta| < 5$ with $p_T < 0.5$ GeV,[3] which contributes to the true $\vec{\not{p}}_T$. In addition to this, mismeasurement of the transverse momenta for jets, leptons, etc. alters the true $\vec{\not{p}}_T$ by an sizable amount. This is due to the finite resolution of detectors and is handled in theoretical predictions by smearing the energy/momentum of a particle through a Gaussian function.

In our study, we have tried to reconstruct $\vec{\not{p}}_T$, taking into account all the above issues. The missing transverse momentum in any event is defined as $\vec{\not{p}}_T = -\Sigma \vec{p}_T^{\text{visible}}$, where the $\Sigma \vec{p}_T^{\text{visible}}$ consists of isolated leptons/photons/jets and also those objects which do not belong to any of these components but are detected at the detector, constituting the so-called "soft part" or the "unclustered component" of the visible momentum. We describe below the various components of the visible $\vec{p}_T$ and their respective resolution functions.

[3]The threshold is 0.5 GeV for CMS and 1 GeV for ATLAS.

3. Resolution effects

Among the finite resolution effects of the detector, taken into account in our analysis, most important are the finite resolutions of the electromagnetic and hadron calorimeters, and the muon track resolution. Since the kind of final state we are dealing with does not require any isolated electrons/photons, we have not considered electron or photon resolution. The electrons/photons which are not isolated but have $E_T \geq 10$ GeV and $|\eta| < 5$ have been considered as jets and their resolution has been parametrized according to that of jets. Jets have been defined within a cone of $\Delta R = 0.4$ and $E_T \geq 20$ GeV using the PYCELL fixed cone jet formation algorithm in PYTHIA. Since the staus are long lived and live a charged track in the muon chamber, their smearing criteria have been taken to be the same as those of isolated muons. Though one can describe the resolution of the track of staus and muons by different resolution functions (as $m_{\tilde{\tau}} \gg m_{\mu}$), one does not envision any significant deviation in the prediction of events via such difference. Therefore, in the absence of any clear guidelines, we have treated them on equal footing, as far as the Gaussian smearing function is concerned. The tracks which show up in the muon chamber, but are not isolated, having $E_T > 10$ GeV and $|\eta| < 2.5$, have been considered as jets and smeared accordingly. All the particles (electron, photon, muon, and stau) with $0.5 < E_T < 10$ GeV and $|\eta| < 5$ (for muon or muonlike tracks, $|\eta| < 2.5$), or hadrons with $0.5 < E_T < 20$ GeV and $|\eta| < 5$, which constitute "hits" in the detector, are considered as soft or unclustered components. Their resolution functions

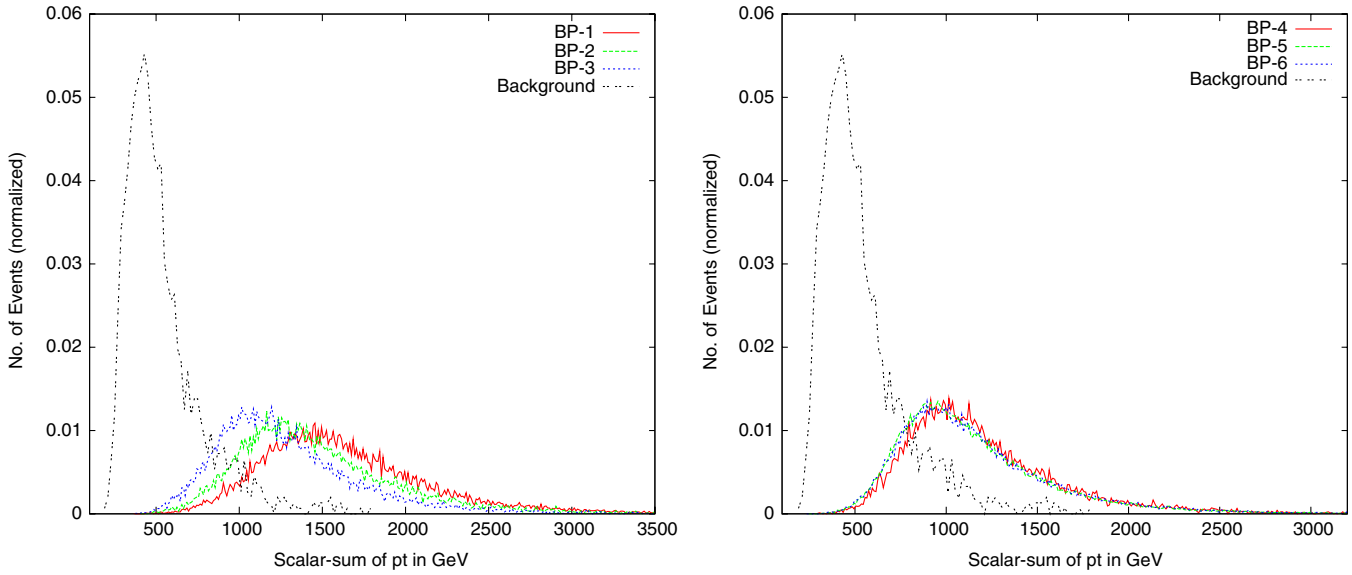

FIG. 2 (color online). $\Sigma|\vec{p}_T|$ distribution (normalized to unity) for the signal and the background, for all benchmark points.

have been considered separately. We present below the different parametrization of the different component of the final state, assuming the smearing to be Gaussian in nature.[4]

Jet energy resolution:

$$\sigma(E)/E = a/\sqrt{E} \oplus b \oplus c/E, \tag{12}$$

where

$$\begin{array}{llll} a = 0.7\ (\mathrm{GeV}^{1/2}), & b = 0.08\& & c = 0.009\ (\mathrm{GeV}), & \text{for } |\eta| < 1.5, \\ = 1, & = 0.1, & = 0.009, & 1.5 < |\eta| < 5. \end{array}$$

Muon/stau p_T resolution:

$$\sigma(p_T)/p_T = a, \quad \text{if } p_T < \xi, \tag{13}$$

$$= a + b\log(p_T/\xi), \quad \text{if } p_T > \xi, \tag{14}$$

where

$$\begin{array}{llll} a = 0.008, & b = 0.037\& & \xi = 100\ (\mathrm{GeV}), & \text{for } |\eta| < 1.5, \\ = 0.02, & = 0.05, & \xi = 100, & 1.5 < |\eta| < 2.5. \end{array}$$

Soft component resolution:

$$\sigma(E_T) = \alpha\sqrt{\Sigma_i E_T^{(\mathrm{soft})i}} \tag{15}$$

with $\alpha \approx 0.55$. One should keep in mind that the x and y components of E_T^{soft} need to be smeared independently and by the same quantity.

It is of great importance to ensure that the stable $\tilde{\tau}$ leaving a track in the muon chamber is not faked by an actual muon arising from a standard model process. As has been mentioned in Sec. I, we have found certain kinematic prescriptions to be effective as well as reliable in this respect. In order to see this clearly, we present the p_T distributions of the harder muon and the $\tilde{\tau}$ track in Fig. 1. The $\tilde{\tau}$-p_T clearly shows a harder distribution, owing to the fact that the stau takes away the lion's share of the p_T possessed by the parent neutralino. Another useful discriminator is the scalar sum of transverse momenta of all detected particles (jets, leptons, and unclustered components). The distribution in $\Sigma|\vec{p}_T|$, defined in the above manner, displays a marked distinction for the signal events, as shown in Fig. 2. The cuts chosen in Table III have been guided by both of the above considerations. They have been applied for all the benchmark points, as also for the background calculation.

IV. NUMERICAL RESULTS AND NEUTRALINO RECONSTRUCTION

A. The reconstruction strategy

Having obtained the τ four-momenta, the neutralinos can be reconstructed, once we obtain the energy of the $\tilde{\tau}$'s

[4]Although a "double Gaussian" smearing is followed in more realistic detector simulations, our illustrative study is now substantially affected by such considerations.

whose three-momenta are already known from the curvature of the tracks in the muon chamber. For this, one needs to know the $\tilde{\tau}$ mass. In addition, the requirements are, of course, sufficient statistics, minimization of errors due to QCD jets faking the τ's, and the suppression of combinatorial backgrounds. For the first of these, we have presented our numerical results uniformly for an integrated luminosity of 300 fb^{-1}, although some of our benchmark points require much less luminosity for effective reconstruction. We have already remarked on the possibility of reducing the faking of τ's. As we shall show below, a systematic procedure can also be adopted for minimizing combinatorial backgrounds to the reconstruction of neutralinos. The primary step in this is to combine each such τ with one of the two hardest tracks in the muon chamber, which satisfy the cuts listed in Table III. A particular τ is combined with a heavy track of opposite charge. However, since neutralinos are Majorana fermions, producing pairs of $\tau^+\tilde{\tau}^-$ and $\tau^-\tilde{\tau}^+$ with equal probability, this is not enough to avoid the combinatorial backgrounds. Therefore, out of the two τ's and two heavy tracks, we select those pairs which give the closer spaced invariant masses, with $|M^{\rm pair1}_{\tilde{\tau}\tau} - M^{\rm pair2}_{\tilde{\tau}\tau}| <$ 50 GeV. The number of signal and background events after the successive application of cuts are listed in Table IV.

This finally brings us to the all-important issue of knowing the stau mass. The $\tilde{\tau}$ mass can be reconstructed from the information on time delay (Δt) between the inner tracker and the outer muon system and the measured three-momentum of the charged track [26]. The accuracy of this method depends on the accurate determination of Δt, which can be limited when the particles are highly boosted. We have followed a somewhat different approach to find the actual mass of the particle associated with the charged track. We have found this method effective when both pairs of $\tau\tilde{\tau}$ come from $\chi^0_1\chi^0_1$ or $\chi^0_2\chi^0_2$.

Solving for the $\tilde{\tau}$ mass: The actual $\tilde{\tau}$ mass can be extracted by demanding that the invariant masses of the two correct $\tilde{\tau}\tau$ pairs are equal, which yields an equation involving one unknown, namely, $m_{\tilde{\tau}}$:

$$\sqrt{m^2_{\tilde{\tau}} + |\vec{p}_{\tilde{\tau}_1}|^2}\cdot E_{\tau_1} - \sqrt{m^2_{\tilde{\tau}} + |\vec{p}_{\tilde{\tau}_2}|^2}\cdot E_{\tau_2} = \vec{p}_{\tilde{\tau}_1}\cdot\vec{p}_{\tau_1} - \vec{p}_{\tilde{\tau}_2}\cdot\vec{p}_{\tau_2}, \quad (16)$$

where the variables have their usual meanings and are experimentally measurable event by event. ($\tilde{\tau}_{1,2}$ here denotes the lighter $\tilde{\tau}$'s on two sides of the cascade, and not the two $\tilde{\tau}$ mass eigenstates.)

The right combination is assumed to be selected whenever the difference between $|M^{\rm pair1}_{\tilde{\tau}\tau} - M^{\rm pair2}_{\tilde{\tau}\tau}|$ is minimum and differs by not more than 50 GeV, as mentioned earlier. It should be noted that the unambiguous identification of the right $\tau\tilde{\tau}$ pairs which come from decays of two neutralinos ($\chi^0_1\chi^0_1$ or $\chi^0_2\chi^0_2$) does not depend on the actual stau mass. Thus we can use a ''seed value'' of the stau mass as input to the above equation, in identifying the right $\tau\tilde{\tau}$ combinations. We have used a seed value of $m_{\tilde{\tau}} \approx$ 100 GeV (motivated by the LEP limit on $m_{\tilde{\tau}}$). The SM background has already been suppressed by demanding the p_T of each charged track to be greater than 100 GeV, together with $\Sigma|\vec{p}_T| > 1$ TeV.

Once the right pairs are chosen using the seed value of the $\tilde{\tau}$ mass, we need not use that value any more, and instead solve Eq. (16) which is quadratic in $m^2_{\tilde{\tau}}$. We have kept only those events in which at least one positive solution for $m^2_{\tilde{\tau}}$ exists. When both roots of the equation are positive, the higher value is always found to be beyond the reach of the maximum center-of-mass energy available for the process. Hence we have considered the solution corresponding to the lower value of the root. The distribution of the solutions thus obtained has a peak around the actual $\tilde{\tau}$ mass. The $\tilde{\tau}$-track four-momenta are completely constructed, using this peak value as the actual mass of the $\tilde{\tau}$ NLSP (see Fig. 3). The fact that these peaks faithfully yield the $\tilde{\tau}$ mass (see Table I) makes it unnecessary to extract this mass from ''fits.''

This sets the stage fully for the reconstruction of neutralinos, the results of which are shown in Fig. 4. For BP1, BP2, and BP3 one can see that there is only one peak which corresponds to the χ^0_1. This is because the χ^0_2 production rate in cascade is relatively small for these points. For BP4 and BP5, on the other hand, we have distinct peaks for both χ^0_1 and χ^0_2. At BP6, however, we only have the χ^0_2 peak. This is due to the small mass splitting between χ^0_1 ($M_{\chi^0_1} =$ 129 GeV) and $\tilde{\tau}$ ($M_{\tilde{\tau}} =$ 124 GeV), which softens the tau (jet) arising from its decay, preventing it from passing the requisite hardness cuts. On the whole, it is clear from Fig. 4 (comparing the peaks with the input values of the neutralino masses) that, in spite of adulteration by QCD jets that

TABLE IV. Number of signal and background events for $2\tau_j + 2\tilde{\tau}$(charged track) + $\not{E}_T + X$ final state with an integrated luminosity of 300 fb^{-1}, considering all SUSY processes. The standard model Higgs mass is taken to be 120 GeV in the background calculation.

Cuts	Signal						Background			
	BP1	BP2	BP3	BP4	BP5	BP6	$t\bar{t}$	ZZ	ZH	Total
Basic cuts	1765	4143	11 726	20 889	28 864	15 439	4129	45	6	4180
$+P_T$ cut	1588	3631	9 471	15 526	20 282	9920	210	3	1	214
$+\Sigma\|P_T\|$ cut	1442	3076	6 777	9 538	11 266	5724	63	0	0	63
$+\|M^{\rm pair1}_{\tilde{\tau}\tau} - M^{\rm pair2}_{\tilde{\tau}\tau}|$ Cut	408	887	1 622	2 004	2 244	858	6	0	0	6

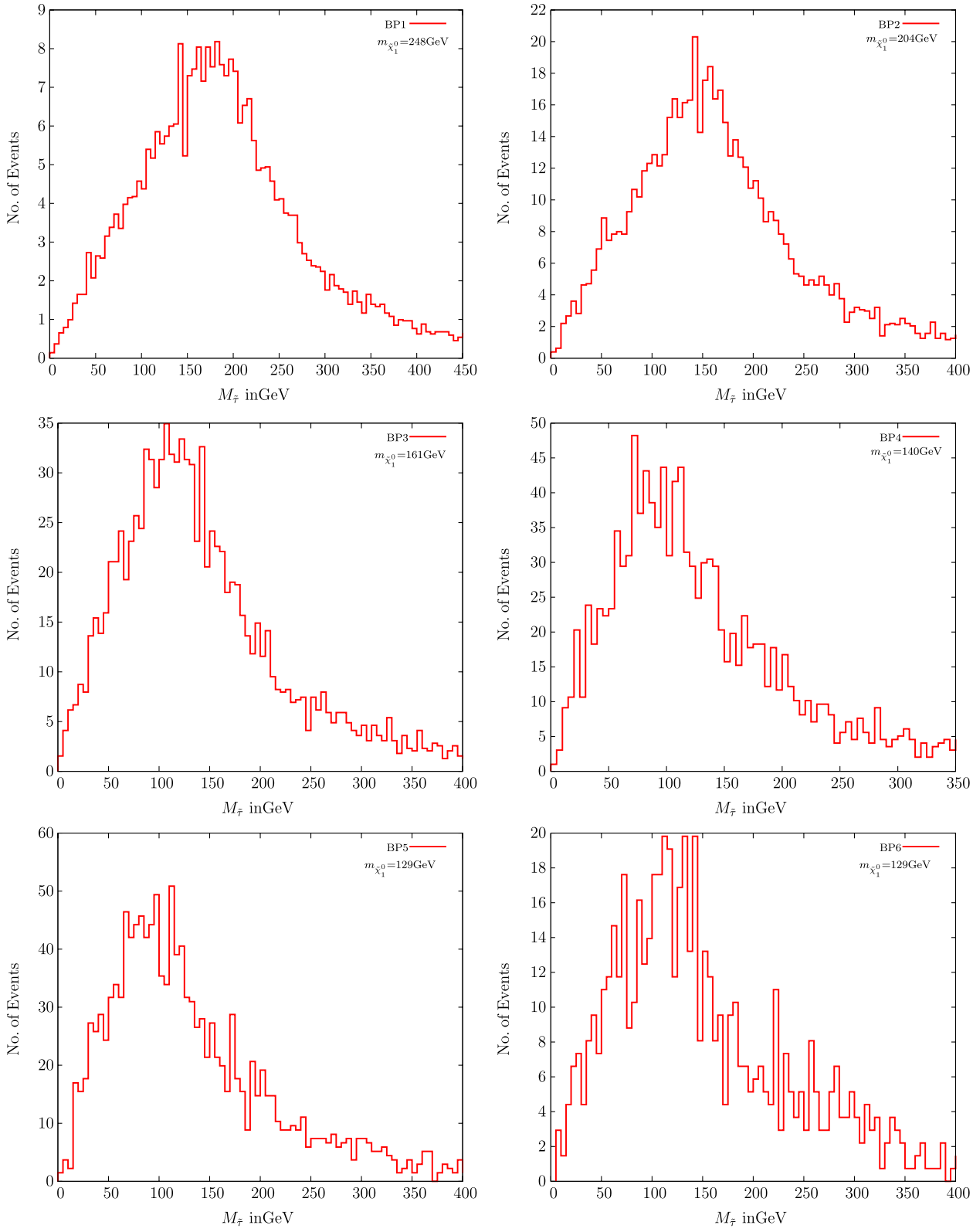

FIG. 3 (color online). The $\tilde{\tau}$ mass peak as obtained from eventwise reconstruction as described in the text, for all the benchmark points at luminosity 300 fb^{-1}.

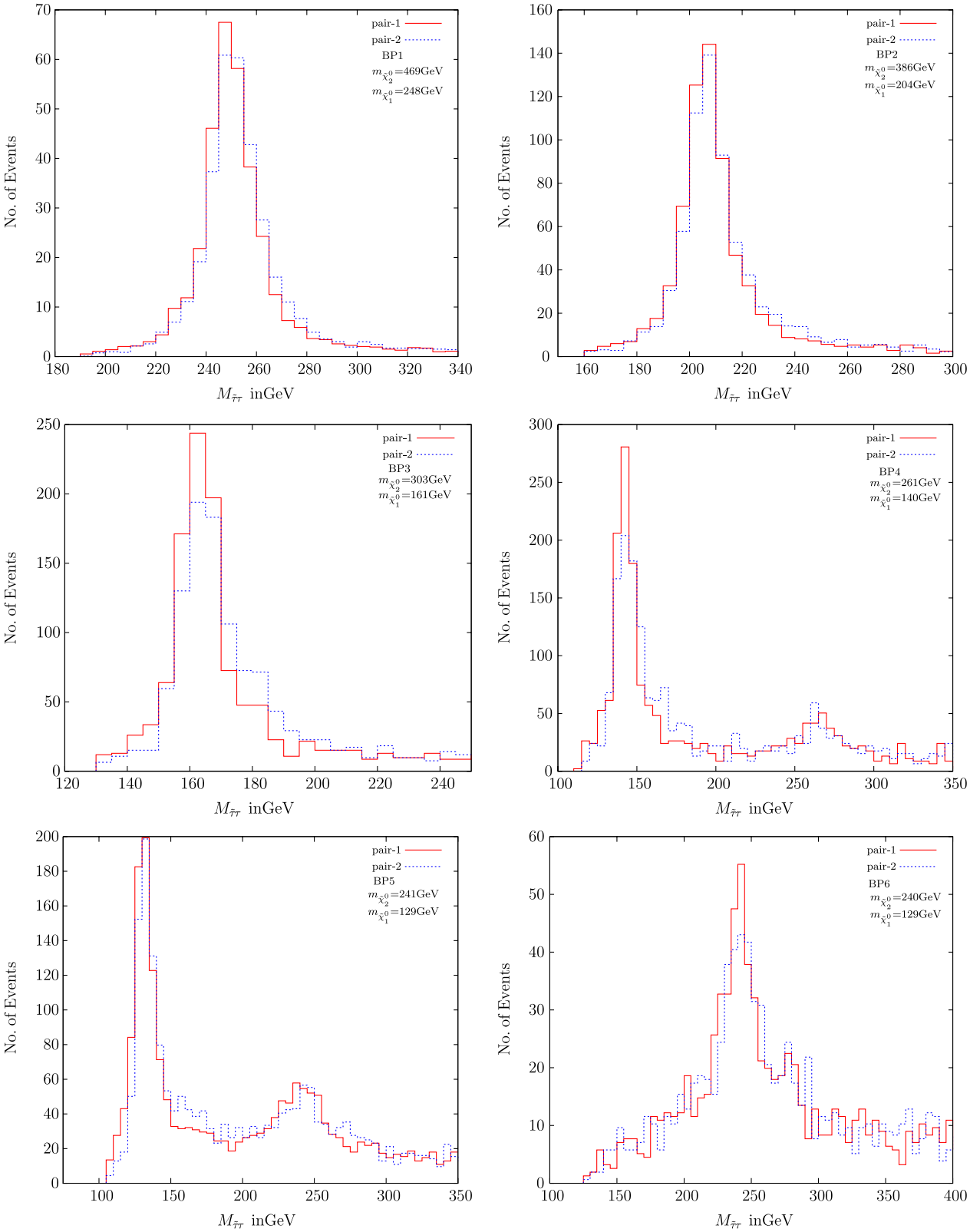

FIG. 4 (color online). $M_{\tilde{\tau}\tau}$ distribution for all the benchmark points at luminosity 300 fb^{-1}. BP1, BP2, and BP3 show only the χ_1^0 peak. Both the χ_1^0 and χ_2^0 peaks are visible for BP4 and BP5, while BP6 displays only the χ_2^0 peak.

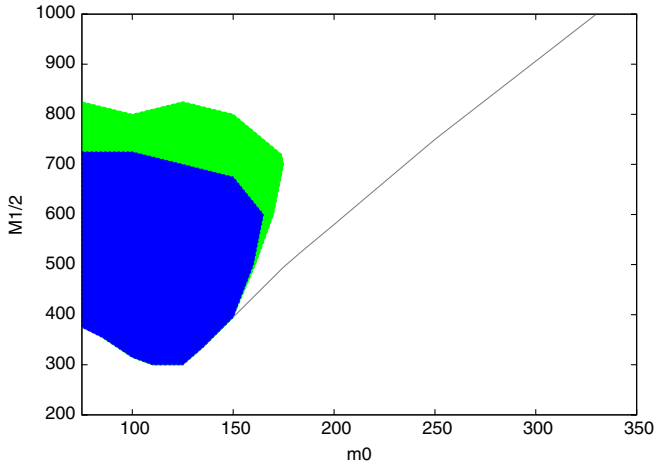

FIG. 5 (color online). The region in the $m_0 - M_{1/2}$ plane, where it is possible to reconstruct at least one of the neutralinos at the LHC, with $\tan\beta = 30$ and $A_0 = 100$. In the dark shaded (blue) region, at least 100 events are predicted in the vicinity of the peak. The additional available region where 50 events in the vicinity of the peak are assumed to suffice for reconstruction is marked as light shaded (green). The entire region above the dashed line indicates the scenario where one has a $\tilde{\nu}_R$ LSP and a $\tilde{\tau}$ NLSP.

fake the τ's, our event selection criteria can lead to faithful reconstruction of neutralino masses.

One may still like to know whether a neutralino reconstructed in this manner is the χ_1^0 or the χ_2^0, when only one peak is visible. This requires further information on the SUSY spectrum. For example, the information on the gluino mass, extracted from the effective mass [defined as $(\Sigma|\vec{p}_T| + \not{E}_T)$] distribution, may enable one to distinguish between the χ_1^0 and the χ_2^0, once gaugino mass unification at high scale is assumed.

B. LHC reach in the $m_0 - M_{1/2}$ plane

We have also identified the region in the $m_0 - M_{1/2}$ plane, where at least one of the two lightest neutralinos can be reconstructed. For this, we have scanned over the region of the $m_0 - M_{1/2}$ plane using the spectrum generator SUSPECT (v 2.34) [31] which leads to a $\tilde{\tau}$ LSP in a usual mSUGRA scenario without the right-handed sneutrino [32]. Results of this scan are shown in Fig. 5. The colored (shaded) areas are consistent with all the low-energy constraints like $b \to s\gamma$, $B_s \to \mu^+\mu^-$, $\Delta(g_\mu - 2)$ and the LEP limits on the low-energy spectrum. The value of $\tan\beta$ has been fixed at 30, and $A_0 = 100$ has been chosen.

The regions where reconstruction is possible have been determined using the following criteria:

(i) In the parameter space, we have not gone into regions where the gluino mass exceeds ≈ 2 TeV.

(ii) The number of events satisfying $|M_{\tilde{\tau}\tau} - M_{\rm peak}| < 0.1 M_{\rm peak}$ at an integrated luminosity of 300 fb^{-1} must be greater than a specific number in order that the peak is said to be reconstructed. One obtains the dark shaded (blue) region if this number is set at 100. If the peak can be constructed from more than 50 events, the additional region, marked as light shaded (green), becomes allowed.

V. SUMMARY AND CONCLUSIONS

We have considered a SUGRA scenario, with universal scalar and gaugino masses, where a right-chiral neutrino superfield exists for each family. We have identified several benchmark points in the parameter space of such a theory, where a right sneutrino is the LSP, and a $\tilde{\tau}$ mass eigenstate is the NLSP. The $\tilde{\tau}$, stable on the distance scale of the detectors, leaves a charged track in the muon chamber, which is the characteristic feature of SUSY signals in this scenario. We use this feature to reconstruct neutralinos in the $\tau\tilde{\tau}$ channel. For this, we use the collinear approximation to obtain the four-momentum of the τ, and suggest a number of event selection criteria to reduce backgrounds, including combinatorial ones. We also suggest that the $\tilde{\tau}$ mass may be extracted by solving the equation encapsulating the equality of invariant masses of two $\tau\tilde{\tau}$ pairs in each event. We find that at least one of the two lightest neutralinos can be thus reconstructed clearly over a rather large region in the $m_0 - M_{1/2}$ plane, following our specified criteria.

ACKNOWLEDGMENTS

We thank Bruce Mellado for his valuable suggestions on several technical points, and Subhaditya Bhattacharya for giving important comments on the manuscript. We also thank Priyotosh Bandyopadhyay, Asesh K. Datta, Nishita Desai, and Sudhir K. Gupta for helpful discussions. This work was partially supported by funding available from the Department of Atomic Energy, Government of India for the Regional Centre for Accelerator-based Particle Physics, Harish-Chandra Research Institute. Computational work for this study was partially carried out at the cluster computing facility of Harish-Chandra Research Institute (http://cluster.mri.ernet.in).

[1] For reviews see, for example, H. E. Haber and G. L. Kane, Phys. Rep. **117**, 75 (1985).
[2] S. Dawson, E. Eichten, and C. Quigg, Phys. Rev. D **31**, 1581 (1985); X. Tata, arXiv:hep-ph/9706307; M. E. Peskin, arXiv:0801.1928.
[3] A. H. Chamseddine, R. L. Arnowitt, and P. Nath, Phys. Rev. Lett. **49**, 970 (1982).
[4] D. Feldman, Z. Liu, and P. Nath, J. High Energy Phys. 04 (2008) 054.
[5] R. N. Mohapatra *et al.*, Rep. Prog. Phys. **70**, 1757 (2007).
[6] T. Schwetz, M. Tortola, and J. W. F. Valle, New J. Phys. **10**, 113011 (2008); G. L. Fogli *et al.*, Phys. Rev. D **78**, 033010 (2008); A. Bandyopadhyay, S. Choubey, S. Goswami, S. T. Petcov, and D. P. Roy, arXiv:0804.4857.
[7] T. Asaka, K. Ishiwata, and T. Moroi, Phys. Rev. D **73**, 051301 (2006); **75**, 065001 (2007).
[8] E. Komatsu *et al.*, Astrophys. J. Suppl. Ser. **180**, 330 (2009).
[9] K. Hamaguchi, M. M. Nojiri, and A. de Roeck, J. High Energy Phys. 03 (2007) 046.
[10] S. K. Gupta, B. Mukhopadhyaya, and S. K. Rai, arXiv:0710.2508.
[11] D. Choudhury, S. K. Gupta, and B. Mukhopadhyaya, Phys. Rev. D **78**, 015023 (2008).
[12] J. L. Feng, A. Rajaraman, and F. Takayama, Phys. Rev. Lett. **91**, 011302 (2003); Phys. Rev. D **68**, 063504 (2003); J. R. Ellis, K. A. Olive, Y. Santoso, and V. C. Spanos, Phys. Lett. B **588**, 7 (2004); J. L. Feng, S. Su, and F. Takayama, Phys. Rev. D **70**, 075019 (2004); A. Ibarra and S. Roy, J. High Energy Phys. 05 (2007) 059.
[13] S. Dimopoulos, M. Dine, S. Raby, and S. D. Thomas, Phys. Rev. Lett. **76**, 3494 (1996); D. A. Dicus, B. Dutta, and S. Nandi, Phys. Rev. Lett. **78**, 3055 (1997); S. Ambrosanio, G. D. Kribs, and S. P. Martin, Phys. Rev. D **56**, 1761 (1997); D. A. Dicus, B. Dutta, and S. Nandi, Phys. Rev. D **56**, 5748 (1997); K. M. Cheung, D. A. Dicus, B. Dutta, and S. Nandi, Phys. Rev. D **58**, 015008 (1998); J. L. Feng and T. Moroi, Phys. Rev. D **58**, 035001 (1998); P. G. Mercadante, J. K. Mizukoshi, and H. Yamamoto, Phys. Rev. D **64**, 015005 (2001).
[14] S. Ambrosanio, G. D. Kribs, and S. P. Martin, Phys. Rev. D **56**, 1761 (1997); A. V. Gladyshev, D. I. Kazakov, and M. G. Paucar, Mod. Phys. Lett. A **20**, 3085 (2005); T. Jittoh, J. Sato, T. Shimomura, and M. Yamanaka, Phys. Rev. D **73**, 055009 (2006).
[15] S. P. Martin, arXiv:hep-ph/9709356, and references therein.
[16] C. Amsler *et al.* (Particle Data Group), Phys. Lett. B **667**, 1 (2008).
[17] S. P. Martin and P. Ramond, Phys. Rev. D **48**, 5365 (1993).
[18] N. Arkani-Hamed, L. J. Hall, H. Murayama, D. Tucker-Smith, and N. Weiner, Phys. Rev. D **64**, 115011 (2001).
[19] C. L. Chou and M. E. Peskin, Phys. Rev. D **61**, 055004 (2000).
[20] A. Djouadi, M. Drees, and J. L. Kneur, J. High Energy Phys. 03 (2006) 033.
[21] F. E. Paige, S. D. Protopopescu, H. Baer, and X. Tata, arXiv:hep-ph/0312045.
[22] T. Sjostrand, S. Mrenna, and P. Skands, J. High Energy Phys. 05 (2006) 026.
[23] H. L. Lai *et al.* (CTEQ Collaboration), Eur. Phys. J. C **12**, 375 (2000).
[24] W. Beenakker, R. Hopker, M. Spira, and P. M. Zerwas, Nucl. Phys. **B492**, 51 (1997).
[25] W. Beenakker, S. Dittmaier, M. Kramer, B. Plumper, M. Spira, and P. M. Zerwas, Nucl. Phys. **B653**, 151 (2003).
[26] I. Hinchliffe and F. E. Paige, Phys. Rev. D **60**, 095002 (1999).
[27] G. Aad *et al.* (The ATLAS Collaboration), arXiv:0901.0512.
[28] D. L. Rainwater, D. Zeppenfeld, and K. Hagiwara, Phys. Rev. D **59**, 014037 (1998).
[29] Y. Coadou *et al.*, ATLAS Internal Note No. ATL-PHYS-98-126.
[30] CMS Collaboration, CERN Report Nos. CMS-TDR-8.1, CERN/LHCC 2006-001.
[31] A. Djouadi, J. L. Kneur, and G. Moultaka, Comput. Phys. Commun. **176**, 426 (2007).
[32] A. V. Gladyshev and D. I. Kazakov, Phys. At. Nucl. **70**, 1553 (2007).